Supporting Information

Polypyrrole-Based Double Rare Earth Hybrid Nanoparticles for Multimodal Imaging and Photothermal Therapy

Xueru Shan[a], Qian Chen[a], Xiangyu Yin[a], Chunzhu Jiang[a], Tinghua Li[a], Shanshan Wei[a], Xinyu Zhang[a], Guoying Sun[a,b,*], Jianhua Liu[c*] and Lehui Lu[d*]

[a.] Jilin Province Key Laboratory of Carbon Fiber Development and Application, School of Chemistry and Life Science, Changchun University of Technology, 2055 Yanan Street, Changchun 130012, P. R. China. E-mail: sunguoying@ccut.edu.cn

[b.] Advanced Institute of Materials Science, Changchun University of Technology, 2055 Yanan Street, Changchun 130012, P. R. China

[c.] Department of Radiology, Second Hospital of Jilin University, Changchun, 130041, P. R. China. E-mail: drliujh@yahoo.com

[d.] State Key Laboratory of Electroanalytical Chemistry, Changchun Institute of Applied Chemistry, Chinese Academy of Sciences, 5625 Renmin Street, Changchun, P. R. China. E-mail: lehuilu@ciac.ac.cn

S1. Experimental section

S1.1. Solubility and Colloidal Stability

PPy@BSA-Gd/Dy NPs were dispersed in water, saline, PBS, Roswell Park Memorial Institute (RPMI-1640), Dulbecco's modification of Eagle's medium (DMEM) and Fetal bovine serum (FBS), respectively. The photos were taken after 24 h.

S1.2. *In Vitro* Hemolysis Assay.

First, 1mL of fresh blood was harvested from ICR mice and washed with PBS by centrifuging at 3000 rpm for 5 min to obtain red blood cells (RBCs). Then, the RBCs were further purified by centrifuging for 5 times and diluted with PBS. Afterward, 1.2 mL of PPy@ BSA-Gd/Dy NPs at different concentrations was mixed with 0.3 mL of RBCs solutions. At the same time, equal volume of PBS and water were used to replace samples for negative and positive control, respectively. Finally, the mixture was maintained at 37℃ for 3h, followed by centrifuging at 3000 rpm for 5 min. The absorbance of the supernatant at 541 nm was measured by UV-vis-NIR. The hemolysis percent of RBCs was calculated by using the following equations:

$$\text{Hemolysis (\%)} = \frac{A_{Sample} - A_{Negative}}{A_{Positive} - A_{Negative}} \times 100\%$$

The A_{Sample}, $A_{Negative,}$ and $A_{Positive}$ were the absorbance of the samples, negative control and positive control, respectively.

S1.3. Intracellular Uptake Assay.

The amount of Gd^{3+} in HeLa cells was also evaluaterd. Cells were cultured in 6-well plates (10^6 per well) for 24 h and then incubated with various concentrations of PPy@BSA-Gd/Dy NPs (0.05, 0.1, and 0.2 mg mL^{-1}) for another 12 h. After that, the cells were washed three times with PBS, trypsinized, lyophilized and digested with HNO_3 (1mL, 10%, v/v). Finally, the intracellular Gd^{3+} concentration was measured by ICP-MS.

S1.4. *In Vivo* Pharmacokinetics

To study the pharmacokinetics behavior, ICR mice were injected with PPy@BSA-Gd/Dy NPs at the Gd^{3+} dose of 5mg mL^{-1} by intravenous administration. About 20 μL

of blood was collected from tail at 10min, 30min, 1h, 2h, 4.5h, 6.5h, 17.5h, 19.5h post-injection, respectively. Then, the samples were treated with aqua regia and the amount of Gd^{3+} was analyzed by ICP-MS.

S1.5. Biodistribution

The biodistribution of PPy@BSA-Gd/Dy NPs was studies on ICR mice. 100 μL of NPs ($[Gd^{3+}]$ = 5mg mL^{-1}) was intravenously injected into the mice. Then, the heart, liver, spleen, lung, and kidney were extracted at the specific time (2 h, 1, 7, 15, 30 days), followed by organs wet weighting, aqua regia treatment and quantification of Gd^{3+} using ICP-MS. On the other hand, urine and feces of each mouse were collected at different time points and dissolved in aqua regia for 48 h.

S1.6. Serum Biochemistry assay.

On the 30 th day, the blood from the eye socket of ICR mice with the intravenous injection of PPy@ BSA-Gd/Dy were collected for blood biochemistry analysis. The healthy mice without any treatment as a control group.

S2. Calculation of photothermal conversion efficiency of PPy@BSA-Gd/Dy NPs

The photothermal conversion efficiency (η) of PPy@BSA-Gd/Dy was calculated using following equations [1,2]:

$$\sum_i m_i C_{p,i} \frac{dT}{dt} = Q_{in,np} + Q_{in,surr} - Q_{out} \quad (1)$$

where m represents the mass of solvent (water) and cuvette, C_p is the heat capacity of solvent (water) and cuvette, T is the solution temperature. $Q_{in,np}$ is the photothermal energy input from the PPy@BSA-Gd/Dy NPs. $Q_{in,surr}$ is the heat absorbed by the solvent (water), which was measured independently to be 25.1mW. Q_{out} is the heat lost to the surroundings.

$Q_{in,np} = I\,(1-10^{(-A_{808})})\eta$ (2)

where I is laser power. A_{808} is the absorbance of NPs at the excitation wavelength of 808nm.

$Q_{out} = hA(T-T_{surr})$ (3)

where h is the heat transfer coefficient, A represents the surface area of the container. T_{surr} is the surrounding temperature.

When the system temperature rises to a maximum steady-state, the rate of heat input is equal to the rate of heat lost to the surrounding.

$Q_{in,np} + Q_{in,surr} = Q_{out} = hA(T_{max}-T_{surr}) = I\,(1-10^{(-A_{808})})\eta + Q_{in,surr}$ (4)

Rearranging eq(4) :

$$\eta = \frac{hA\,(T_{max} - T_{surr}) - Q_{in,surr}}{I\,(1 - 10^{-(A_{808})})} \quad (5)$$

In equal (5), only hA is unknown for calculating η.

In order to get the hA, θ as a dimensionless driving force temperature is introduced:

$$\theta = \frac{T - T_{surr}}{T_{max} - T_{surr}} \quad (6)$$

In the absense of any laser excitation, eq (1) becomes

$$\sum_i m_i C_{p,i} \frac{dT}{dt} = -Q_{out} = -hA(T - Tsurr) \quad (7)$$

τ_s is introduced as a sample system constant:

$$\tau_s = -\frac{\sum_i m_i C_{p,i}}{hA} \quad (8)$$

Integrating eq (6), (7) and (8):

$$t = -\frac{\sum_i m_i C_{p,i}}{hA} \ln\theta \quad (9)$$

As shown in Fig.2f, τ_s=295.04s

$$hA = \frac{1\times 4.2 + 2\times 0.839}{295.04} = 0.020$$

$$\eta = \frac{hA\,(T_{max} - T_{surr}) - Q_{in,surr}}{I\,(1 - 10^{-(A_{808})})}$$

$$= \frac{0.020\times 27\times 1000 - 25.1}{2000\times(1 - 10^{-1.8})}\times 100 = 26.16\%$$

S3. Supplementary Figures

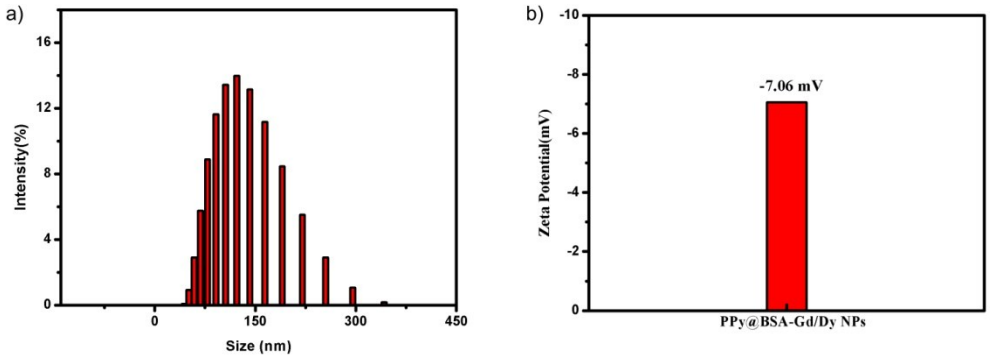

Fig.S1. a) Hydrodynamic size and b) Zeta potential of PPy@BSA-Gd/Dy NPs.

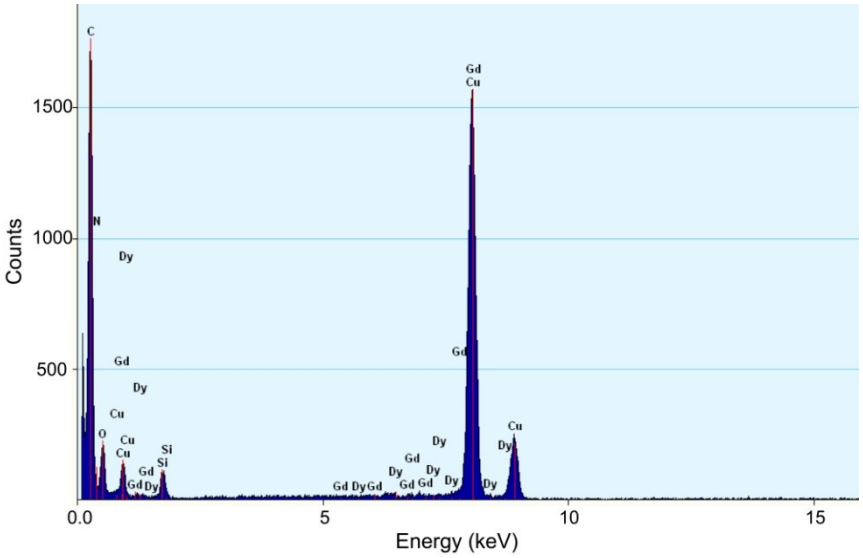

Fig.S2. EDS of PPy@BSA-Gd/Dy NPs.

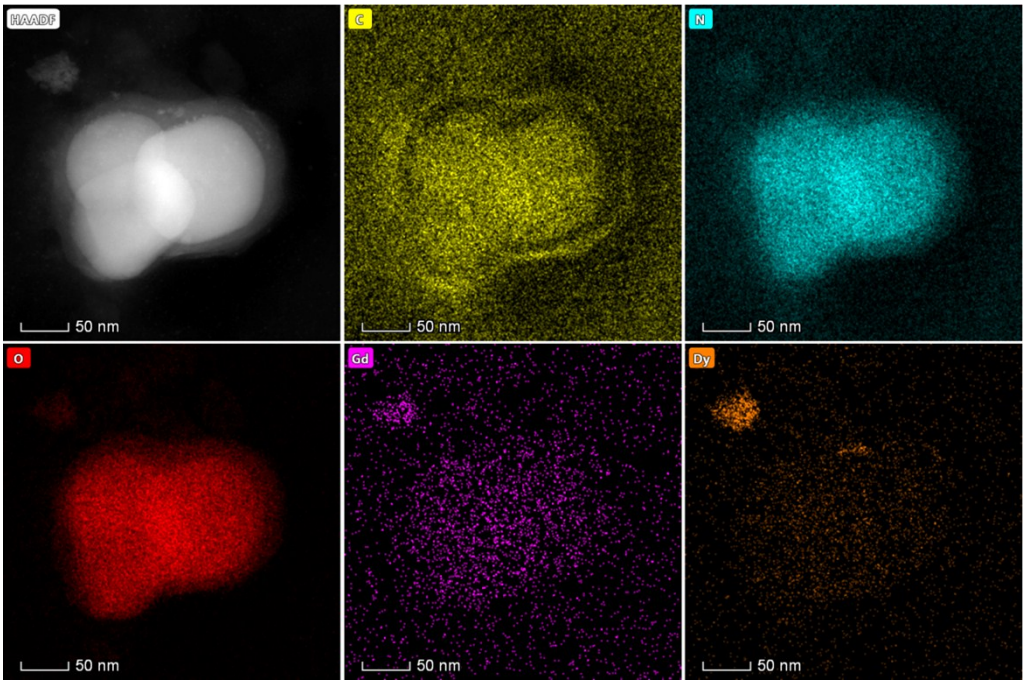

Fig.S3. High-angle annular dark-field (HAADF)-STEM and elemental mapping of PPy@BSA-Gd/Dy NPs.

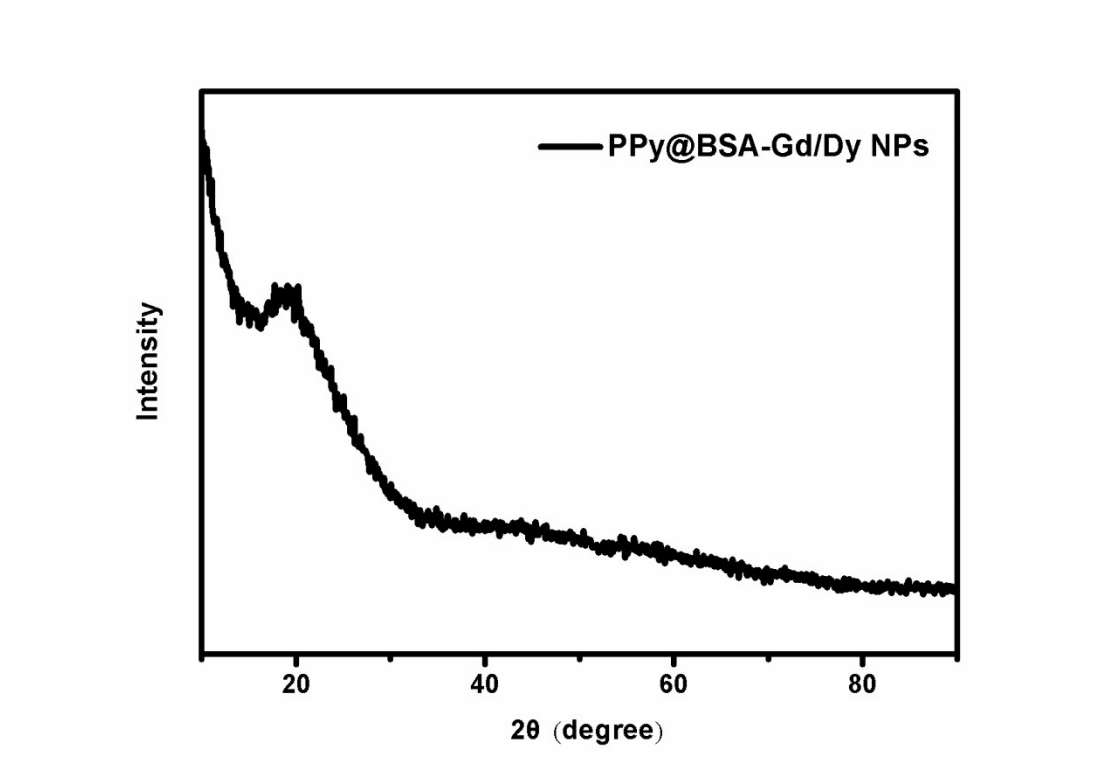

Fig.S4. XRD spectrum of PPy@BSA-Gd/Dy NPs.

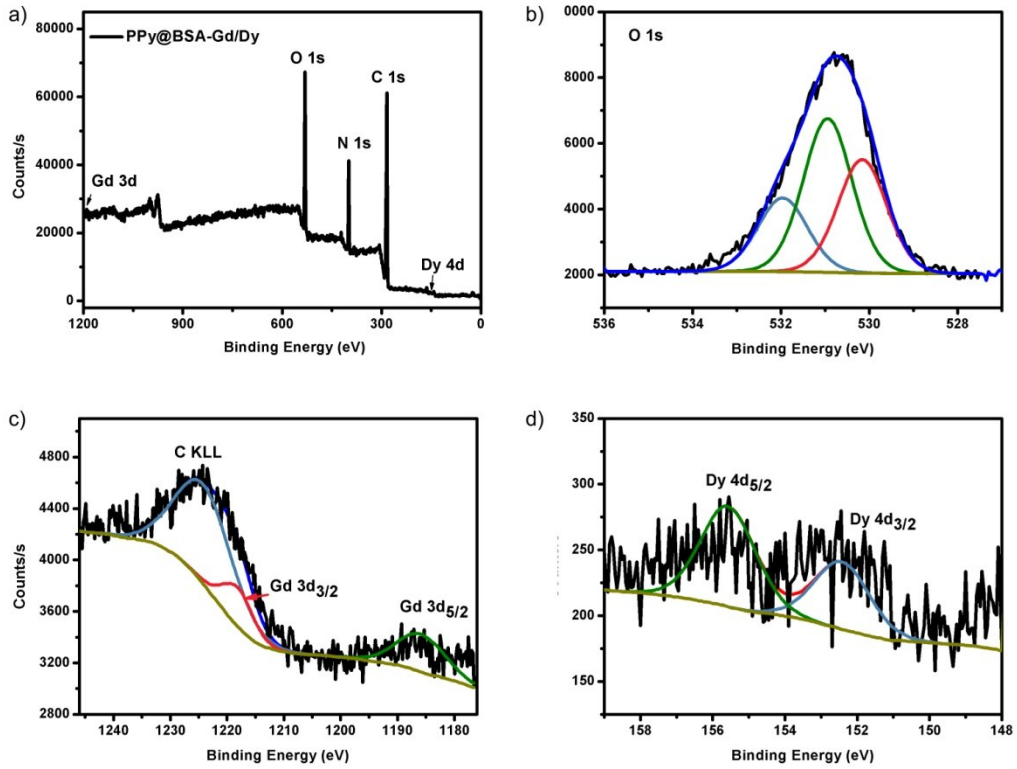

Fig.S5. a) The XPS survey spectrum of PPy@BSA-Gd/Dy NPs. The selective XPS survey spectrum corresponding to b) O element c) Gd 3d spectra: Gd^{3+} $3d_{5/2}$ at 1186.5 eV,Gd^{3+} $3d_{3/2}$ at 1219.0 eV, and d) Dy 4d spectra of PPy@BSA-Gd/Dy NPs: Dy^{3+} $4d_{5/2}$ at 152.5 eV, Dy^{3+} $4d_{3/2}$ at 155.7 eV.

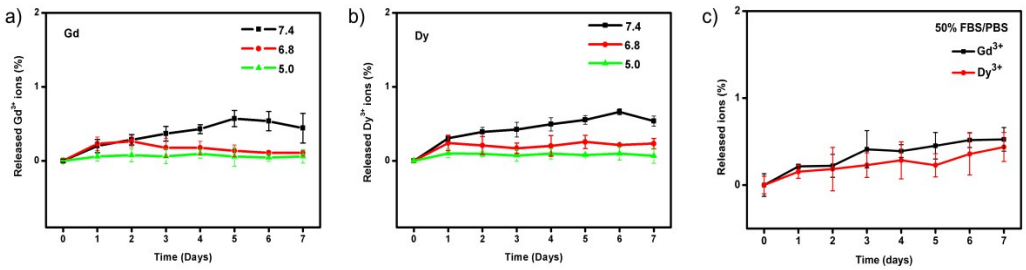

Fig.S6. a) The Gd^{3+} leakage test and b) Dy^{3+} leakage test of PPy@BSA-Gd/Dy NPs in PBS with different pH. c) The Gd^{3+} / Dy^{3+} leakage test of PPy@BSA-Gd/Dy NPs in 50% FBS/PBS for 7 days.

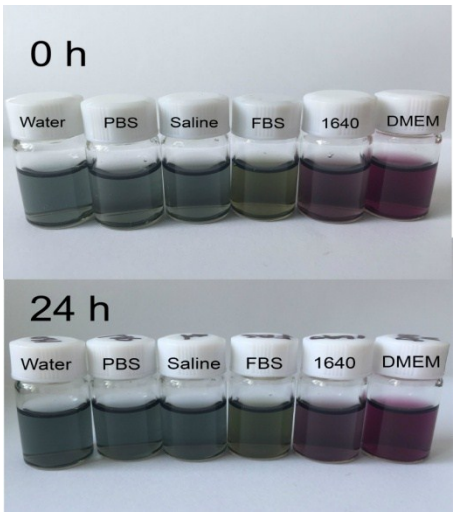

Fig.S7. Photos of PPy@BSA-Gd/Dy NPs, which dispersed in various media including water, PBS, saline, fetal bovine serum (FBS), Roswell Park Memorial Institute (RPMI-1640), and Dulbecco's modification of Eagle's medium (DMEM) for 24 h.

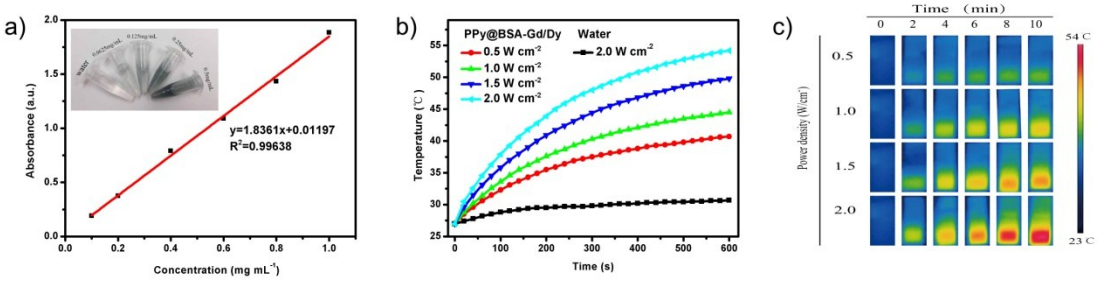

Fig.S8. a) Linear relationship of the absorbance of NPs at 808nm versus the concentration of PPy@BSA-Gd/Dy NPs. b) Photothermal heating curves and c) thermal IR images of NPs at different laser power density upon the same NPs concentrations for 10 min.

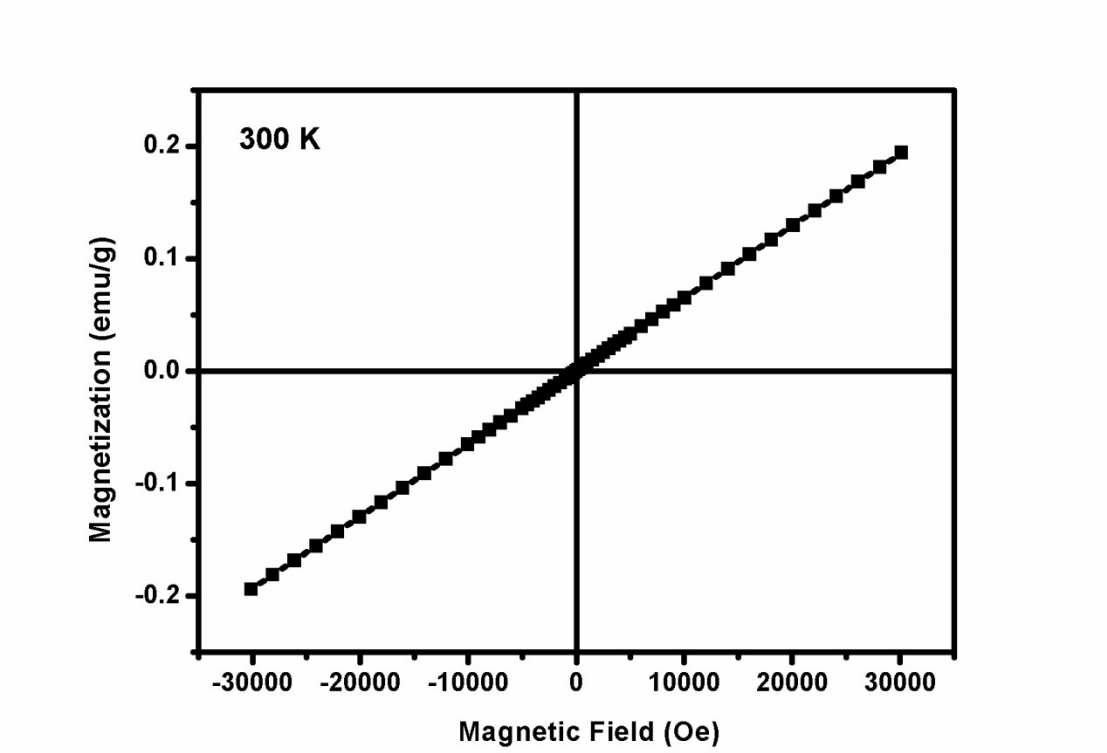

Fig.S9. Magnetic hysteresis loop of the PPy@BSA-Gd/Dy NPs.

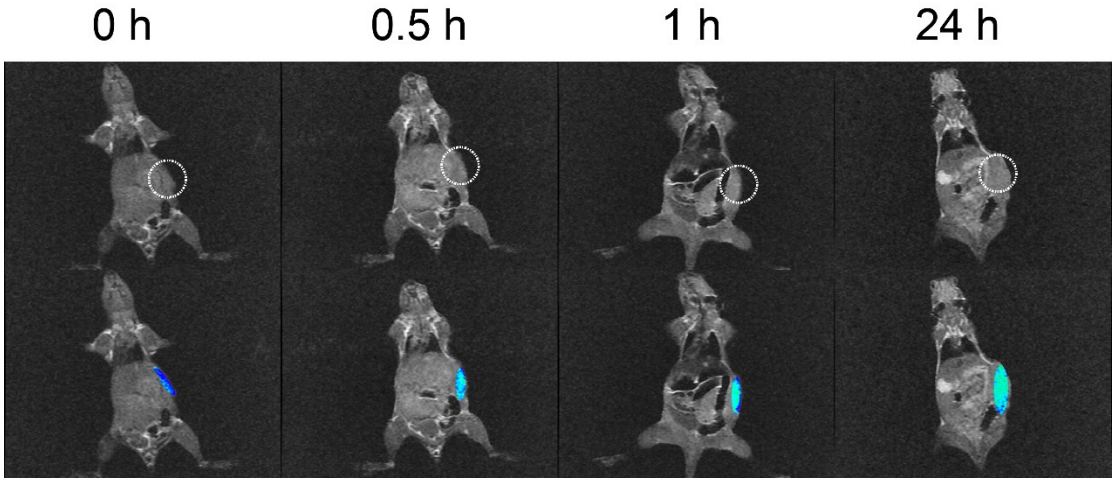

Fig.S10. *In vivo* T_1-weighted MR imaging of tumor-bearing mice after intravenous injection of PPy@BSA-Gd/Dy NPs (100 μL, $[Gd^{3+}]$ = 5 mg mL^{-1}).

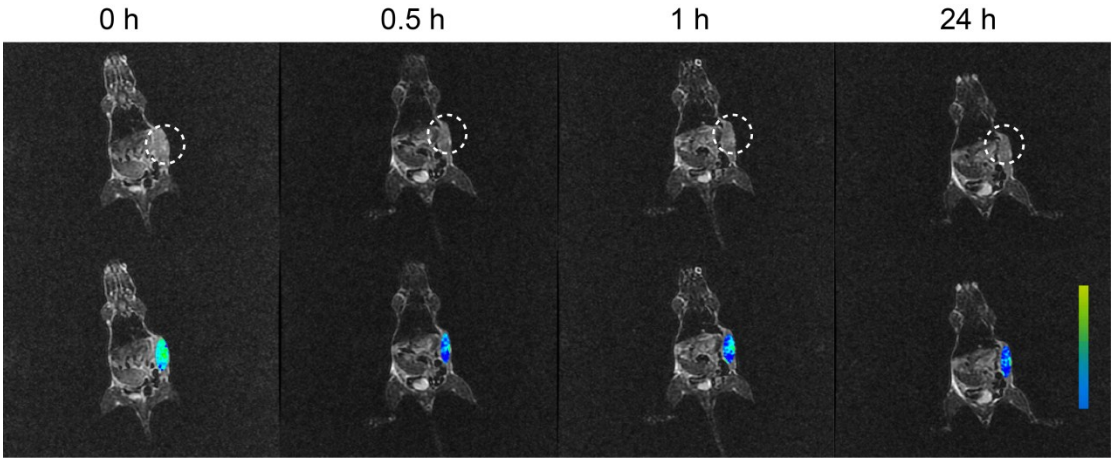

Fig.S11. *In vivo* T_2-weighted MR imaging of tumor-bearing mice after intravenous injection of PPy@BSA-Gd/Dy NPs (100 μL, $[Dy^{3+}]$ = 5 mg mL^{-1}).

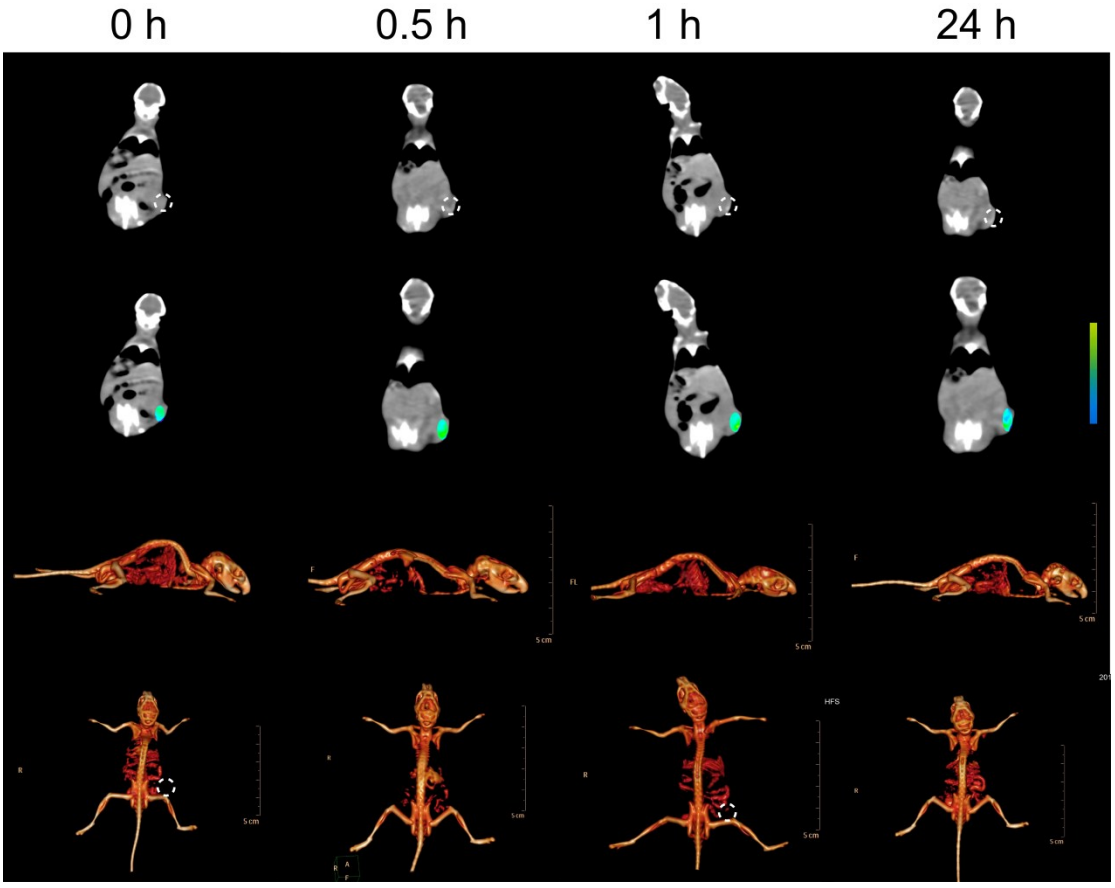

Fig.S12. CT images of tumor-bearing mice after intratumor injection of PPy@BSA-Gd/Dy NPs (40 μL, $[Dy^{3+}]$ = 5 mg mL^{-1}).

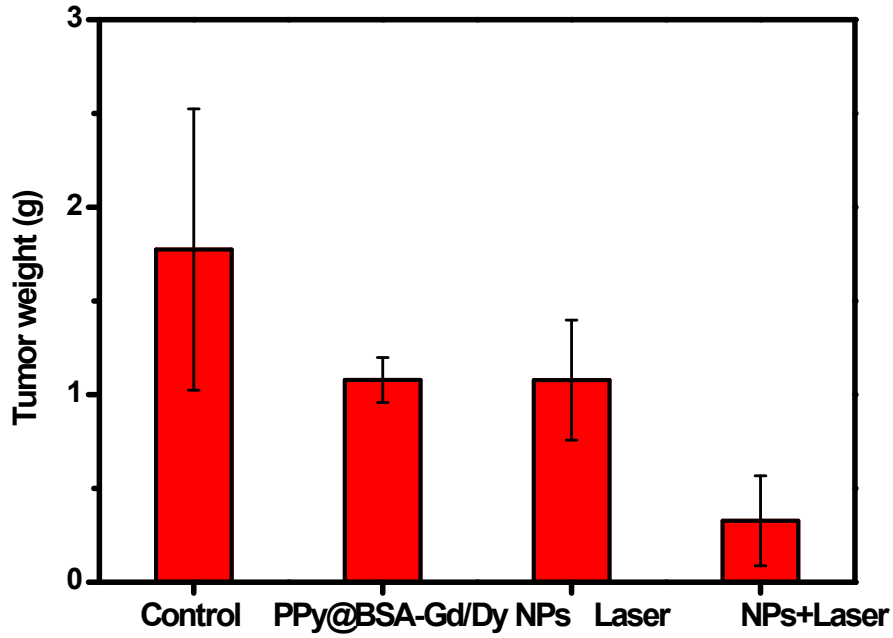

Fig.S13. Tumor weight of mice at different treatment groups.

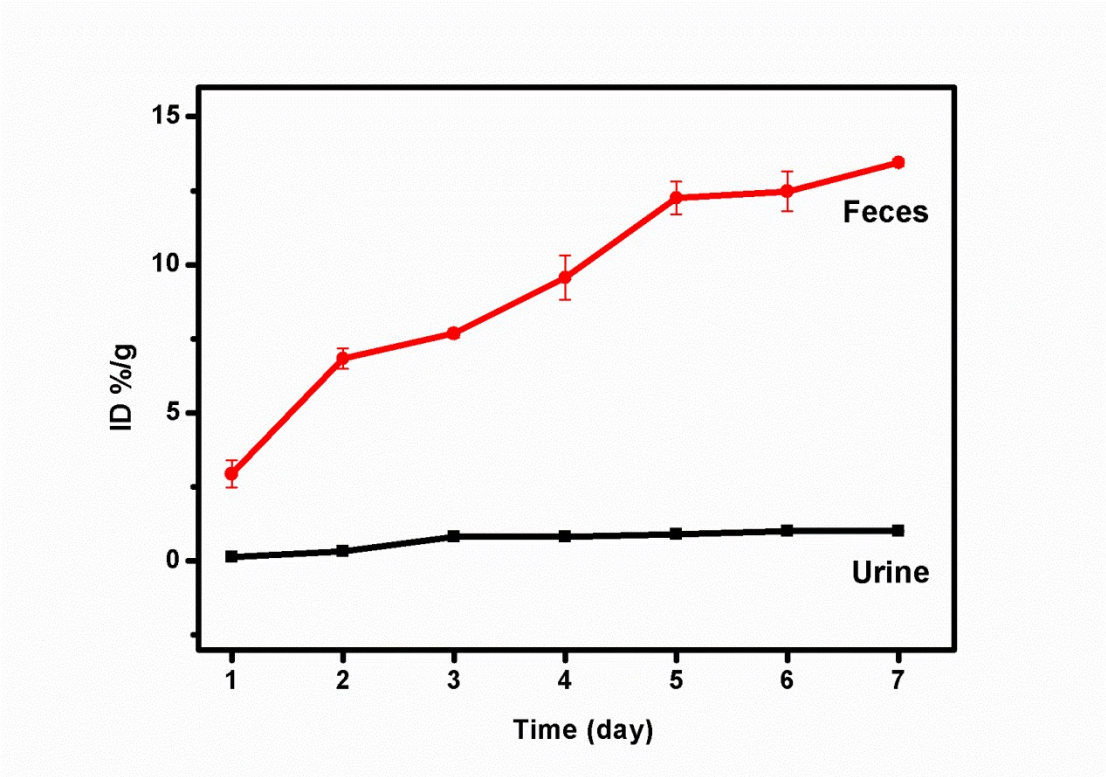

Fig.S14. PPy@BSA-Gd/Dy NPs in urine and feces collected at various time points after injection.

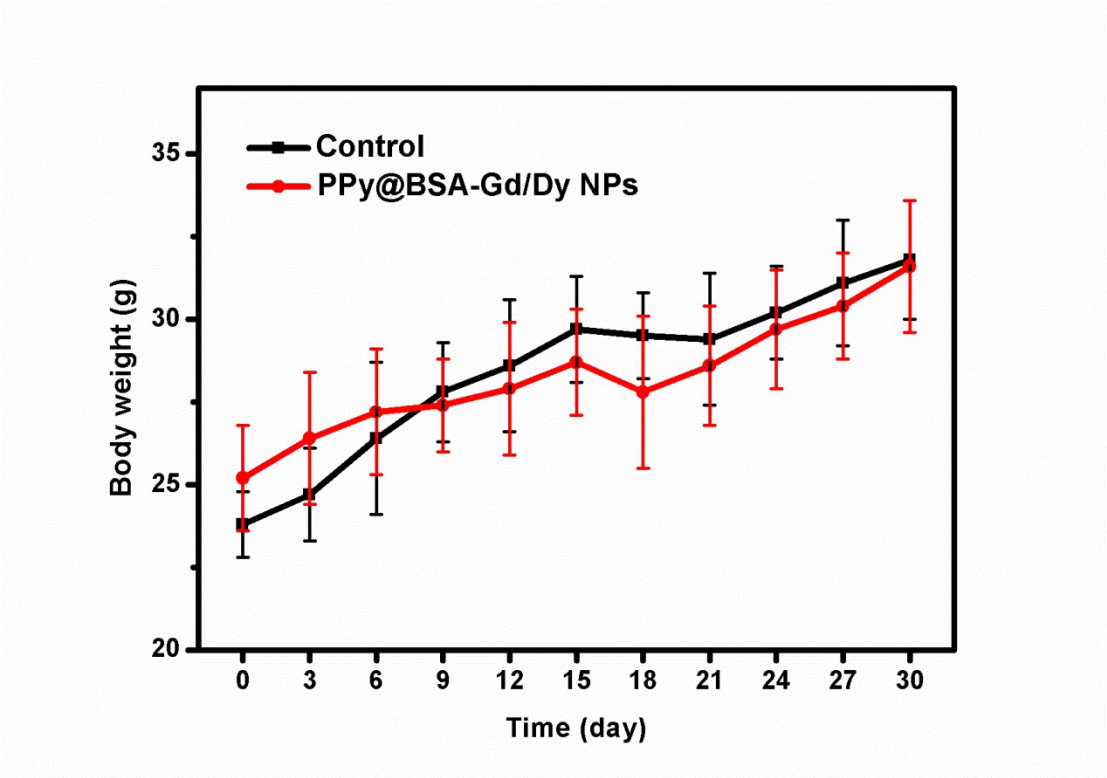

Fig.S15. Body weight changes of the mice with and without intravenous injection of PPy@BSA-Gd/Dy NPs.

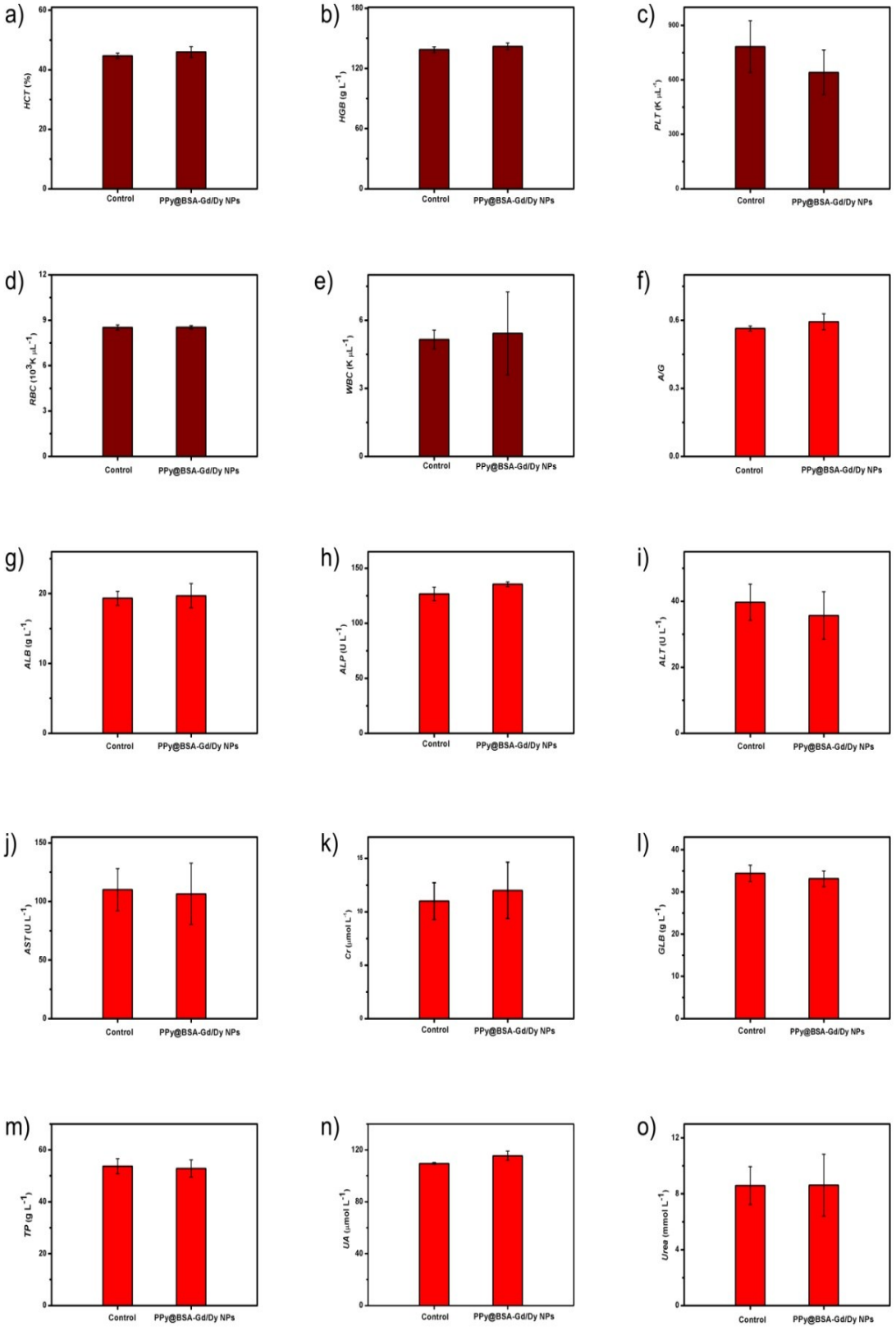

Fig S16. Blood analysis. (a–e) Hematology analysis and (f–o) serum biochemistry detection after intravenous injection of PPy@BSA-Gd/Dy NPs at 30 d.

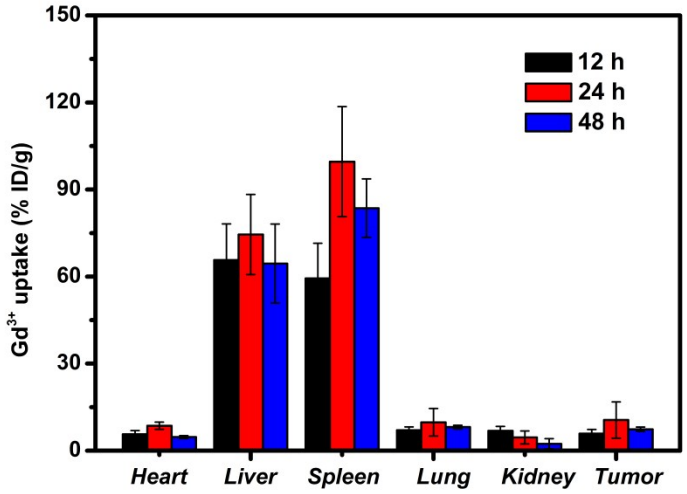

Fig.S17. Biodistribution of the PPy@BSA-Gd/Dy NPs in tumor-bearing mice.

Table S1. Stoichiometric and actual molar ratio of Gd/Dy in PPy@BSA-Gd/Dy NPs.

Stoichiometric molar ratio of Gd/Dy	4:1	2.33:1	1.5:1	1:1
Actual molar ratio of Gd/Dy	2.73:1	1.62:1	1.05:1	1:1.56

References

1. W. He, K. Ai, C. Jiang, Y. Li, X. Song and L. Lu, *Biomaterials*, 2017, **132**, 37-47.
2. W. Zhen, Y. Liu, L. Lin, J. Bai, X. Jia, H. Tian and X. Jiang, *Angew. Chem. Int. Ed.*, 2018, **57**, 10309-10313.